Title

Abstract

ABSTRACT ABSTRACT ABSTRACT

1. Introduction

Recent advances in computational biology have been driven by the development of experimental techniques that generate large datasets and corresponding machine learning algorithms for data analysis and interpretation.

Mass cytometry is a particularly exciting modern technique that allows researchers to measure more than fifty molecular properties of millions of individual cells per experiment (). Researchers can identify cell population heterogeneities ranging in scope from individual cells to complex hierarchical subpopulations. Such precision enables more detailed studies of many medically relevant phenomena, including identifying individual cells in specific disease states (), classifying cellular subpopulations by response to signalling perturbations (), understanding cellular reprogramming processes (), and investigating the natural heterogeneity of healthy systems ().

However, the effectiveness of mass cytometry as an experimental tool depends on correctly interpreting the resulting high-dimensional datasets. To assist with data interpretation, researchers develop machine learning algorithms to calculate summary statistics or generate low-dimensional visualizations of raw data. In the case of mass cytometry, researchers are typically interested in three main analysis tasks, each corresponding to a machine learning task:

Analysis Goal	**Machine Learning Task**	**Example Application**
Identifying and characterizing rare cellular subtypes	Clustering	Identifying minimal residual disease
Describe relations between cellular subtypes	Structured output prediction	Monitoring clonal evolution in cancer
Create human-readable representations to aid interpretation	Low-dimensional embedding	Generating visual summaries for clinicians

Preliminary work. Under review by the International Conference on Machine Learning (ICML). Do not distribute.

Several domain-specific algorithms have been developed to address these analysis tasks, most notably SPADE (), FLOW-MAP (), Wanderlust (), DREMI/DREVI (), and viSNE (). However, some limitations of these algorithms indicate the need for improved solutions. First, none of these methods can be easily related to an underlying probabilistic model. This makes them prone to unpredictable structure-distorting behavior which can lead to misleading outputs. Second, these methods do not quantify how confident researchers should be when using the result to support experimental conclusions.

Here, we investigate SPADE, a widely used mass cytometry analysis algorithm, and comment on its inconsistencies when applied to generated datasets with known ground truth (§2). This analysis indicates that SPADE may generate inaccurate results when applied to real datasets, suggesting the need for improvements. We also propose an alternative algorithm to perform density estimation for the density-dependent downsampling component of SPADE (§3) that results in more accurate downsamplings with greater stability over its parameter space. Finally, we describe an alternative approach to producing low-dimensional embeddings under constraints simlar to those assumed by existing cytometry analysis algorithms (§**??**). MORE ABOUT APPROX TPE.

2. SPADE Inconsistency Analysis

SPADE, or Spanning-tree Progression Analysis of Density-normalized Events () is a popular and influential algorithm for automating cell sub-population identification and visualization, directly from high-dimensional raw datasets.

SPADE (Figure 1) consists of the following multi-step data processing pipeline:

1. **Density Dependent Downsampling**: This simultaneously reduces computational load, and also ensures that rare cell sub-populations are not overshadowed by dominant larger cell clusters.

2. **Clustering** The downsampled data is then used as input for agglomerative clustering, which groups individual cells in the dataset into sub-populations.

3. **Cluster-preserving Up-sampling** Data omitted during downsampling is then assigned to identified sub-

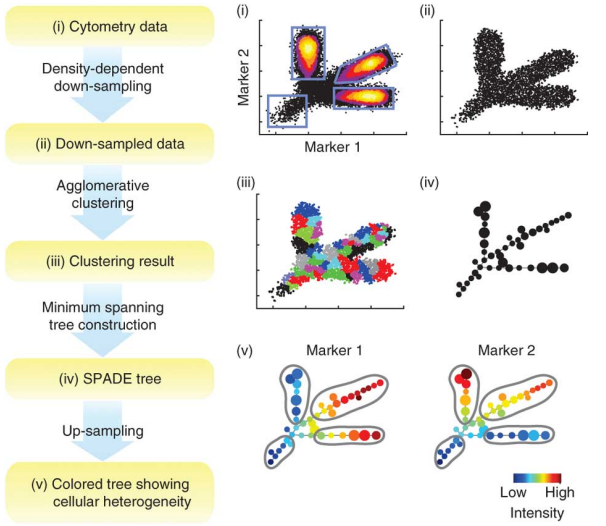

Figure 1. Overview of steps involved in the SPADE algorithm: Density-dependent downsampling, clustering, cluster preserving up-sampling, Minimum Spanning Tree construction, 2-D visualization. Figure from ().

population clusters by a k-nearest-neighbors classifier.

4. **Minimum Spanning Tree Construction** To better understand relations between different subpopulations, a complete graph is constructed on the data with each cluster represented by its centroid and edge weights corresponding to Euclidean distance. A minimum spanning tree is then computed on this underlying graph to pinpoint clusters which are especially close to each other.

5. **Two Dimensional Embedding** To further aid visualization, the minimum spanning tree is then embedded in two dimensions using force-directed layout (). A plot of this embedding is then generated as the final output of SPADE.

While SPADE is a significant improvement over previous manual data analysis techniques, we are concerned that its sub-component algorithms and ad-hoc parameter settings may lead to inconsistent and potentially misleading outputs. Because biologists interpret SPADE visualizations to support or refute hypotheses, it is important that SPADE and related cytometry analysis algorithms yield reproducible results and do not inject structure into visualizations that do not exist in the raw data.

We examined the behavior of SPADE by generating synthetic datasets and comparing their known ground-truth structure to SPADE output visualizations. Figure 2 presents the results of this analysis for a particular 2-dimensional dataset with clear spatial structure. Nine consecutive runs

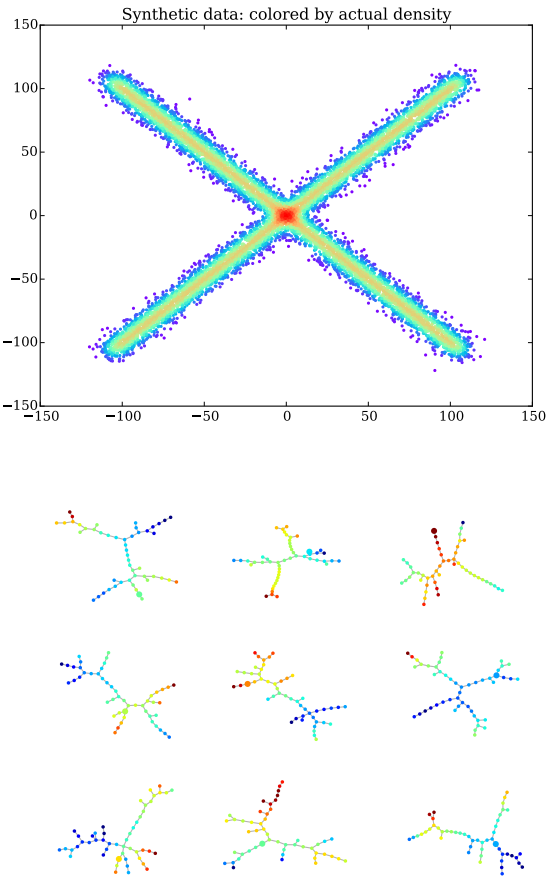

Figure 2. Results of running 9 identical instances of SPADE (*bottom*) on a 2-dimensional synthesized dataset (*top*).

of SPADE on this dataset with the same parameters yielded the visualizations shown—all with wildly different trees and nont with the clear "X" shaped structure present in the input data.

This example, which corroborates with the results of similar analyses (not shown), indicates that SPADE performs inconsistently and inaccurately on even simple synthetic datasets. SPADE's inability to recover the structure of simple constructed example data makes us hesitate to trust its visualizations on much more complex single-cell data. The popularity of SPADE as a general-purpose cytometry analysis tool for a wide range of experiments means that it should be much more robust to variations in input data than our experiments indicate.

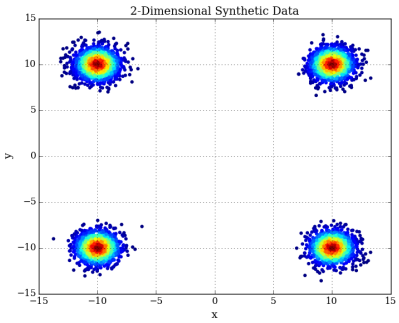

Figure 3. Example 2-dimensional synthetic dataset generated for density estimation algorithm analysis. Point color corresponds to "ground truth" local density.

3. Density-Dependent Downsampling

Both SPADE and FLOW-MAP algorithms for analyzing mass cytometry data involve density-dependent downsampling as a step in the data processing pipeline. This entails randomly omitting a subset of data points such that the probability of omitting a given point is positively correlated with the points local density in the full dataset. Density-dependent downsampling is intended to serve two purposes: First, it should increase the sensitivity to small clusters in successive clustering steps. Second, it should reduce computation cost of subsequent steps by reducing the overall number of points passed to the rest of the algorithm.

Density-dependent downsampling requires a way to estimate the local density at a point p, $D(p)$, to determine the probability of including p in the sampled subset. SPADE and FLOW-MAP estimate $D(p)$ by counting the number of points within a threshold L1-distance r of p. However, this density estimation technique is inadequately justified.

To compare the accuracy of multiple density estimation algorithms, we performed numerical experiments with generated synthetic datasets. First, we drew 5000 points from a scikit-learn kernel density estimator () fit to distinct cluster centers in 2, 10, and 50 dimensions (e.g. Figure 3). The ground truth local density for each point was calculated by scoring the points using the fit kernel density estimator. We then compared these ground truth densities to the output of four potential density estimation algorithms:

1. **Radius Threshold, L1:** The density estimation technique used by SPADE and FLOW-MAP. For each point p, the local density $D(p)$ is estimated as the count of points within a threshold L1-distance r of p.

2. **Radius Threshold, L2:** Identical to 1, except using $L2$ distance for the radius threshold r.

3. **K-Nearest Neighbor, L1:** For each point p, find the k points closest to p by $L1$ distance. The average normalized distance, d, between p and each of these k points in m dimensions transformed as $\exp(d^m)$ (to improve linearity) is the estimated local density $D(p)$.

4. **K-Nearest Neighbor, L2:** Identical to 3, except using $L2$ distance to find nearest neighbors.

Figure 4 shows algorithm performance for a range of parameter values r and k measured as the Spearman correlation coefficient ρ of the predicted density versus the ground truth density. Specific results of interest are the maximum ρ value for each algorithm (indicating the approximate maximum accuracy of the algorithm on this particular dataset), the range of parameter values corresponding to high ρ coefficients, and the general trend of the ρ values over the parameter space.

Both the Radius Threshold and K-Nearest Neighbor density estimators have maximum ρ values near 1 in all three dimensions. However, the K-Nearest Neighbor estimator provides stably accurate estimates with k ranging from $< 2\%$ to 20% of the number of points in the dataset, while the accuracy of the Radius Threshold estimator peaks in a narrow range of values of r. This stability to parameter setting would make the K-Nearest Neighbor estimator a better choice for algorithms such as SPADE and FLOW-MAP. This is especially true considering the difficulty of choosing an appropriate value of r or k given an experimental dataset. Unlike the synthesized datasets used for algorithm analysis, cytometry datasets input to SPADE and FLOW-MAP do not come with a "ground truth" density. SPADE arbitrarily chooses r to be a user-selected parameter α times the median 1-nearest neighbor distance between a randomly selected subset of 2000 data points. Using this heuristic on our synthesized datasets corresponds to the grey dotted lines in Figure 4. While this heuristic works for the 10 dimensional case, it clearly results in a suboptimal density estimation in 2 and 50 dimensions, and we have no reason to believe it generalizes to arbitrary datasets. The K-Nearest Neighbor estimator avoids this "needle in a haystack parameter selection problem.

Figure 4 also indicates that using $L1$ distance results in a wider range of high-accuracy values of r for the Radius Threshold estimation algorithm, but that the choice of distance metric does not have a major effect on density estimation accuracy for the K-Nearest Neighbor algorithm. This further supports the stability of the K-Nearest Neighbor algorithm.

To demonstrate that replacing the Radius Threshold density estimator with the K-Nearest Neighbor estimator would improve the behavior of SPADE, we performed density dependent downsampling using both estimators (WHICH

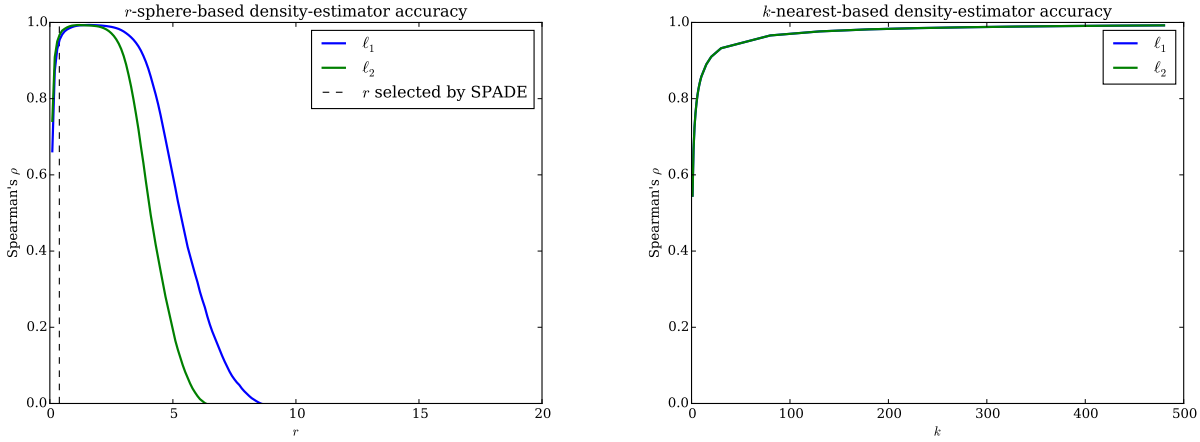

(a) 2-Dimensions

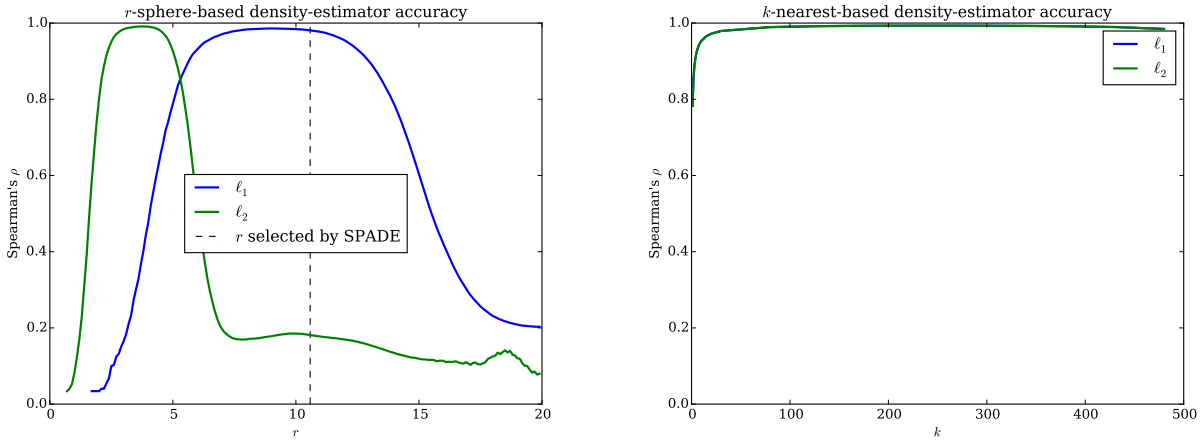

(b) 10-Dimensions

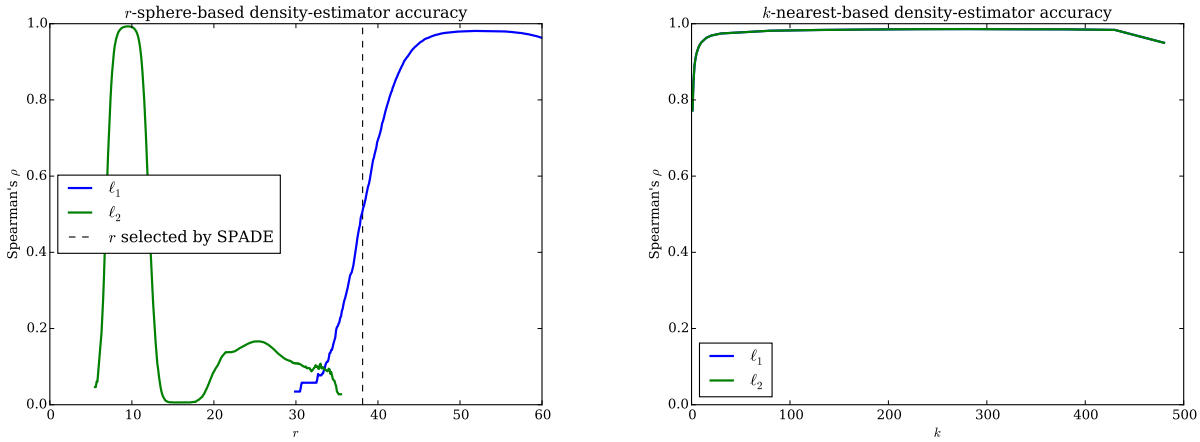

(c) 50-Dimensions

Figure 4. Spearman correlation coefficients of predicted density to ground-truth density using the Radius Threshold (r-sphere) and K-Nearest Neighbors density estimators on synthesized datasets in 2, 10 and 50 dimensions over a range of r and k parameter values. Higher correlation correficients indicate a higher accuracy predicted density.

DISTANCE?) on a synthesized dataset (Figure 5). Notice that Radius Threshold estimator downsampling results in "clumps" of high density (red) points in random locations that do not correspond to high-density clusters in the original data. In comparison, K-Nearest Neighbor estimator downsampling results in a much more uniform sampled dataset which is a better representation of the origial to pass to successive components of the algorithm.

4. Approximate Tree-Preserving Embedding

Background / motivation A primary motivation for creating a 2D embedding is to reveal cluster structure in an intuitive, human-readable representation. Ideally, such an embedding simultaneously preserves clusters and the relations between clusters—similar items within a cluster should be near each other, similar clusters should be close together in the embedding, etc. There are many ways to produce such an embedding, including linear methods like principal component analysis (PCA), and nonlinear methods like Isomap (), Locally Linear Embedding (), and t-SNE (). PCA can be shown to minimize the sum of squared reconstruction errors, which induces an embedding that preserves the largest pairwise distances with high fidelity, and places less emphasis on preserving the smallest pairwise distances. In cases where the clusters are linearly separable in the target dimensionality, the embedding produced by PCA is a suitable visualization. Because clusters are often not linearly separable in real data, nonlinear methods have been developed. Techniques like Isomap and Locally Linear Embedding construct neighborhood graphs and preserve distances (e.g. shortest-path distances) within these graphs, so they can sometimes outperform PCA at local neighborhood preservation and other metrics. However, they may distort or introduce structure not present in the original data, and are sensitive to user-defined settings of free parameters.

Recent work (**?**) constructively produces a low-dimensional embedding such that the results of hierarchical clustering are identical in the original data and the embedding. The Tree-Preserving Embedding algorithm achieves strong theoretical guarantees, but its cost is cubic in the size of the input dataset n (with large leading constants), is prohibitively slow when $n > 300$, and is somewhat complicated to implement correctly.

Here we attempt to develop a simpler low-dimensional embedding technique that also approximately preserves both fine- and coarse-grained cluster structure.

Algorithm We propose Approximate TPE, a simpler approximation that is also naively $O(n^3)$, but provides a more direct route to further performance optimization. Approximate TPE (1) computes an agglomerative hierarchical clus-

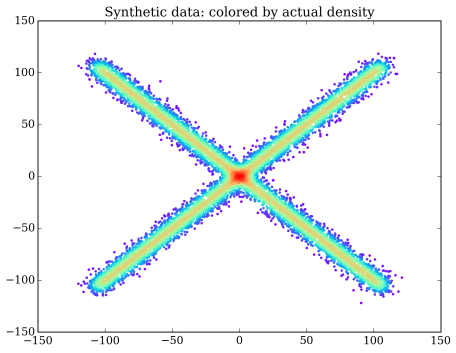

(a) Synthetic Dataset

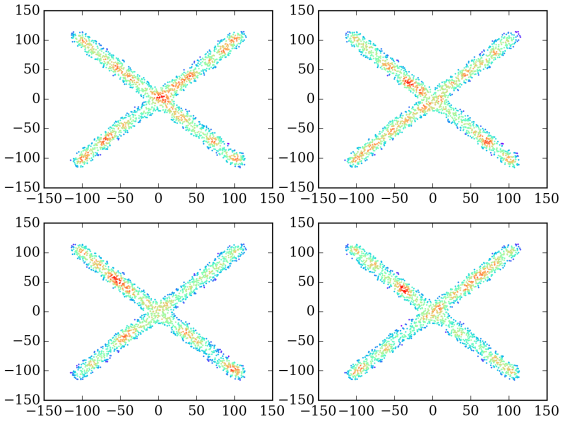

(b) Downsampled with Radius Threshold density estimation

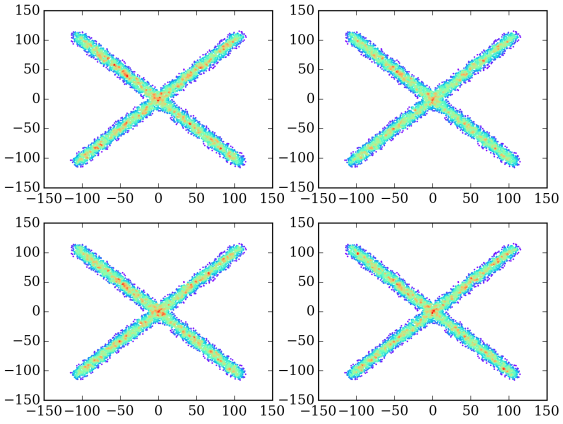

(c) Downsampled with K-Nearest Neighbor density estimation

Figure 5. Comparison of density dependent downsampling on a sample dataset (*top*) performed with the Radius Threshold density estimation algorithm (*middle*) and the K-Nearest Neighbor density estimation algorithm (*bottom*).

ter tree, (2) extracts a pairwise distance matrix A from this tree, and (3) approximately preserves these distances in a low-dimensional embedding. The user can select any linkage to construct the cluster tree (we show results for single-, median-, average, ward-, and complete- linkage). The entries A_{ij} of the pairwise distance matrix are cophenetic distances: the height in the cluster tree at which points i and j are merged. A low-dimensional embedding that approximately preserves these distances is then computed by multidimensional scaling (MDS) ().

Comparison on benchmark data We tested the method on (1) two Gaussians, (2) Gaussians on hypercubes, (3) handwritten digit data ($n = 1797$), (4) ???.

This approximation outperforms competing algorithms when measured by neighborhood preservation.

Competing algorithms: PCA, KPCA (RBF kernel), t-SNE, Isomap, LLE. All with target-dimensionality of 2.

However, depending on the choice of linkage, sometimes the algorithm collapses many similar points into small, dense regions of the embedding, which is visually unreadable. [propose solutions? e.g. we might be able to solve this by rescaling the entries of the cophenetic distance matrix? tried a couple different things: one thing that works is to scale by the Euclidean distance see comment] Two functional approaches to tackling this problem: (1) rescale smallest distances in input matrix (for example, replace smallest distances with raw Euclidean distances), (2) after MDS embedding has been computed, tweak the locations such that very small distances are high-stress: i.e. push apart any pair of points thats too close together

[to-do: measure of tree-preserving-ness]

[to-do: procrustes analysis on synthetic data]

[to-do: measure cluster-preservation somehow? Estimate number of clusters in original data and and low-dimensional embedding and compare?]

[to-do: apply to biological data]

Future work Future work will address the computational cost of the algorithm and the crowding problem, as well as providing better heuristics for choosing the linkage type.

Construction of the hierarchical cluster tree is naively an $O(n^3)$ operation, but that can be reduced to nearly linear-time by bootstrapping with a tree that is much cheaper to construct (such as a KD-tree) (**?**). Another approach to accelerate construction of the cluster tree is to use a sparse k-nearest-neighbors graph (**?**).

Computing a low-dimensional embedding from the distance matrix via MDS is also naively $O(n^3)$, but there has been some research into fast approximations for MDS. $O(n \log n)$ divide-and-conquer approach: http://www.cs.ucla.edu/ weiwang/paper/CIMCV06.pdf Nystrom approaches: FastMap, MetricMap, Landmark MDS

[expand this section?]

5. FLOW-MAP

Recent work proposed FLOW-MAP as an algorithm for 2D visualization of the results of mass cytometry data with a time component. In these experiments, a population of cells is sampled at several time intervals, yielding a series of snapshots of the population over time. The paper introducing FLOW-MAP examined three techniques for stem cell reprogramming. The combined 2D map should illustrate whether the three techniques vary in their end-points / the intermediate cellular states visited by the population over the course of the procedures. In other words, we would like to learn a progression axis for each reprogramming technique that describes the progression of the cellular population over time, and we would like to produce an accurate 2D representation of the data. The authors of the algorithm recognize that the combination of stochastic down-sampling and imposition of very sparse constraints on the final visualization can lead to inconsistency in the results of SPADE. To address these limitations, they proceed by constructing a denser constraint graph, where nodes are clusters and edges are distances between cluster centers. Sparsity is induced by a series of rules for whether an edge should be included in the graph. Edges are further filtered by adjacency in time: two datapoints can only share an edge in this graph if they were observed in either the same time step or in consecutive timesteps. The visualization coordinates are then computed by applying force-directed layout to this slightly denser graph. However, this approach raises some fresh concerns. For example, imposing the constraint of timestep adjacency may obscure the presence of populations that are present at multiple time points that are not adjacent, since they cannot be connected directly by edges. Other constraints imposed by user-defined parameters make it likely for many points to be connected in chains, where each points degree is 2: when combined with force-directed layout, this makes the embedding seem to contain well separated clusters with intermediates stretched along a thin line between them. It is unclear if this is an accurate depiction of the data. To test whether these methods are distorting the data, we need to compare the results obtained using these methods to the results obtained from using simpler methods that are easier to reason about. To this end we cast the problem as a supervised problem: from a cellular feature vector predict what time it was measured. If we can perform this task well, then we have probably learned a good progression function.

References